Original scientific paper

Informacije MIDEM
Journal of Microelectronics, Electronic Components and Materials
Vol. 45, No. 2 (2015), 110 – 116

An influence of the selected factors on the transient thermal impedance model of power MOSFET

Krzysztof Górecki, Janusz Zarębski, Damian Bisewski

Gdynia Maritime University, Department of Marine Electronics, Gdynia, Poland

Abstract: The paper presents the results of experimental studies that illustrate the influence of the selected factors, i.e. the size of soldering pads, the PCB copper area, heat-sink size as well as the dimensions and material of the housing on the transient thermal impedance model parameters of MOSFET. Measurements of thermal parameters were performed using the indirect electrical method. Parameters of the transient thermal impedance model were calculated using the estimation procedure elaborated by the authors. The obtained results show an influence of the system cooling parameters on thermal parameters of the semiconductor device.

Keywords: thermal phenomena; transient thermal impedance; compact thermal model

Vpliv določenih faktorjev na tranzienten termično impedančen model močnostnega MOSFET

Izvleček: Članek predstavlja eksperimentalne rezultate vplivov določenih faktorjev, kot so velikost spajkalnih površin, področje bakra na PCB, velikost hladilnika in velikost ohišja, na tranzienten termično impedančni model MOSFET. Meritve temperaturnih parametrov so bile opravljene s pomočjo posredne električne metode. Parametri tranzientnega modela so bili določeni na osnovi ocenjevalne procedure avtorjev. Rezultati kažejo vpliv hladilnih parametrov sistema na termične parametre elementa.

Ključne besede: termičen pojav; termična impedanca; kompakten termičen model

* *Corresponding Author's e-mail: gorecki@am.gdynia.pl*

1 Introduction

One of the essential phenomena influencing properties of semiconductor devices is self-heating [1, 2, 3, 4, 5]. It appears with a rise of the semiconductor device internal temperature T_j and it is caused by the exchange of electrical energy dissipated in these devices into heat at not ideal cooling conditions. The rise of the device internal temperature causes changes in the course of their characteristics [1, 2, 3] and strongly influences their reliability [6 - 11]. In order to limit the excess of the device internal temperature as a result of self-heating, proper cooling systems are used [12 – 14]. Except of classical systems of free space cooling, systems of forced cooling are also applied. This group of cooling systems includes microchannel cooling systems [15], thermoelectric cooling systems [16] or water cooling systems [17].

An increase in the power density dissipated in modern semiconductor chips causes, that a development of non-typical cooling methods are used, for example - the microchannel heat-sinks [18, 19]. In order to assure efficient electrical insulation between the case of semiconductor device and its heat-sink, different interface materials are applied. Properties of materials are analyzed among others in the paper [20].

Heat removal to the surrounding is realised by three mechanisms [21, 22]: conduction, convection and radiation. The efficiency of these mechanisms depends, among others on the value of the device internal temperature and on the difference between temperature of the device case and the surrounding. In addition, as shown in the papers, e.g. [23, 24], heat transport from the device structure to the surroundings is carried out using a number of paths. Therefore, one should expect this efficiency to undergo some change connected with the changes of the power dissipated in these devices and changes of the manner of their mounting.

Thermal parameters describing the efficiency of removing the heat generated in the semiconductor device to the surrounding are transient thermal impedance $Z_{th}(t)$ and thermal resistance R_{th}. The first of the mentioned parameters describes thermal properties of the device during the transient state, whereas the other one – at the steady-state. Transient thermal impedance $Z_{th}(t)$ of the electronic device is of the form [1, 3, 4, 25]

$$Z_{th}(t) = R_{th} \cdot \left[1 - \sum_{i=1}^{N} a_i \cdot \exp\left(-\frac{t}{\tau_{thi}}\right)\right] \quad (1)$$

where τ_{thi} is the *i*-th thermal time constant, a_i – weighting factor of thermal time constant, N – a number of time constants.

Constructors of semiconductor device cases develop new structures characterized by a low value of thermal resistance between the junction and the case of the semiconductor device [24]. This factor of complex thermal resistance junction-to-ambient, however, is not dominant. In turn, the designers of the cooling system of a semiconductor device should include all external parts of the heat flow path. As it was shown, among others in the papers [25-30], the influence of such factors, as the dissipated power, the mounting method and the ambient temperature on the waveform of transient thermal impedance of the device can be important. As it is shown, e.g. in the papers [25, 26, 31] the value of thermal parameters can change essentially under the influence of such factors, as e.g. lengths of leads and the area of pads.

On the other hand, the computer analysis of electronic networks needs to use computer models of the devices existing in this network. The accuracy of the obtained results of calculations depends on the accuracy of the used models. In order to take into account self-heating phenomena in computer analyses, the compact thermal models of electronic devices are typically used. Parameters values of such model (see Eq. (1)) are dependent on among others construction of the cooling system as well as location of the semiconductor device bias point [23, 30, 31].

In the paper [31] the influence of the selected factors on thermal resistance of semiconductor devices is considered and some formulas describing this influence are proposed. In turn, in the papers [2, 30, 32] it is shown, that the waveforms of transient thermal impedance of semiconductor devices depend on power dissipated in these devices. Unfortunately, the results of measurements presented in the cited papers refer to selected semiconductor devices and cooling systems. Therefore, it is justified to carry out systematic research on the influence of the selected factors on both the waveforms of transient thermal impedance and parameters values of the thermal model for a single semiconductor device at different cooling conditions. SMD Power MOS transistor type IRFR420 contained in DPAK TO-252, was arbitrary chosen for investigations.

In section 2 the used measurement set is described. The considered cooling systems are presented in section 3. The measurement results of the waveforms of transient thermal impedance of the considered device with the values of parameters describing such waveforms are shown in section 4.

2 The measuring set

Transient thermal impedance is determined using the indirect electrical method described in [32]. In this method, the cooling curve [28] of the transistor is measured, whereas the voltage on the forward biased body diode Db of the transistor DUT is used as a thermally-sensitive parameter. The measurements performed by the authors show, that the thermometric characteristic $v_D(T)$ describing the dependence of the forward voltage of the body diode on temperature of the transistor at the constant body diode current I_M=1 mA is linear in the range of temperature from 25 to 110°C. Measurements are realized in three steps using the measurement set shown in Fig.1. At first, the calibration of the characteristics $v_D(T)$ is carried out. Next, heating of the tested transistor operating in the saturation range is realized. This step of measurement is finished, when the device thermally steady state is achieved. The cooling step starts at time t = 0, when the transistor is switched off and the body diode is forward biased by the current I_M.

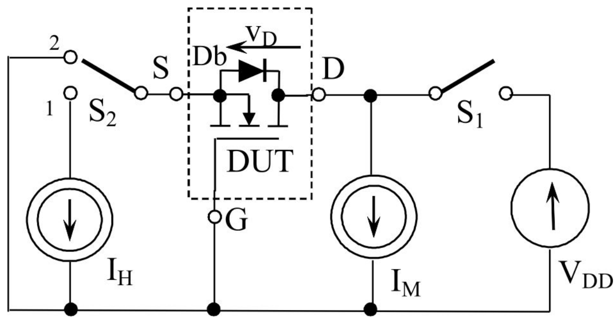

Figure 1: The diagram of the measurement set to measure transient thermal impedance of the power MOSFET

In the measuring set, the source I_M forces the measuring current of the body diode located inside the transistor (DUT). The voltage source V_{DD} and the current source I_H set the dissipated power while the heating. Switches S_1 and S_2 are controlled by the PC. As the switches S_1 and S_2 the power MOS transistors are used. The position of the switches depends on the measurement step. In calibration and cooling, the switch S_1 is open and the switch S_2 is in position 2. While heating, the switch S_1 is closed and the switch S_2 is in position 1. The values of the voltage and current of the DUT are recorded using a 16-bit A/D converter USB-1608GX-2AO manufactured by Measurement Computing. Maximum sampling rate of the converter is equal to 500 kS/s.

3 Cooling systems

Using the measurement system presented in Section 2, transient thermal impedance of the considered power MOS transistor at different set of the cooling system, were measured. The first group of measurements results relates to the transistor mounted on one of the PCBs, where the path mosaic of each PCB is shown in Fig. 2. The black color in Fig. 2 represents areas of PCB covered with the layer of copper. The dimensions of all PCBs are 51 x 33 mm. As seen, the PCB A1 contains copper in the solder pads and conductive paths, only, whereas the PCBs A2 and A3 are covered with additional layers of copper supporting the heat dissipation process. The PCB A2 differs from the PCB A3 in the path width. The considered transistor was soldered, in turn, to each PCB and the silicon insulating spacer and thermal grease, were used. For comparison, the measurements were also performed for the transistor soldered directly to the wires (without the PCB). This variant of assembly is designated by acronym A0.

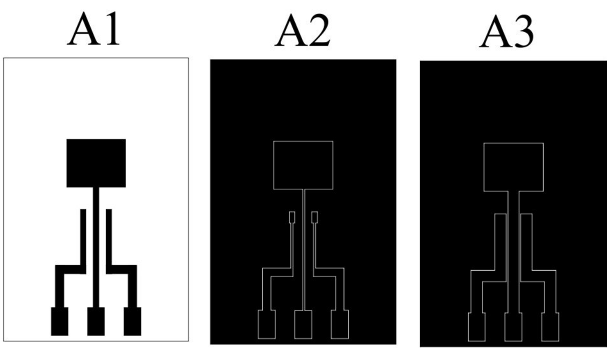

Figure 2: PCBs used for investigations

The second group of measurements relates to the same transistor mounted on the aluminum heat-sink (type A-5723 of the length 100 mm). The measurements were performed for the heat-sink situated in free space (FS) and five types of housings, i.e.: metal housing (ME1) of the dimensions 120 x 220 x 195 mm (volume of about 5 litres), metal housing (ME2) of a dimensions 225 x 115 x 345 mm (10 liters), plastic enclosure (PE1) of a dimensions 170 x 85 x 70 mm (1 litre), plastic enclosure (PE2) of a dimensions 140 x 85 x 170 mm (2 liters) and plastic enclosure (PE3) of the dimensions 225 x 210 x 85 mm (4 litres).

4 Results

The influence of the transistor dissipated power, mounted on the PCB A1, on the waveform of transient thermal impedance is shown in Fig. 3. The values of $Z_{th}(t)$ model parameters for 3 arbitrary chosen values of the dissipated power are presented in Table 1. These values were determined using the estimation procedure ESTYM, proposed by the authors [32].

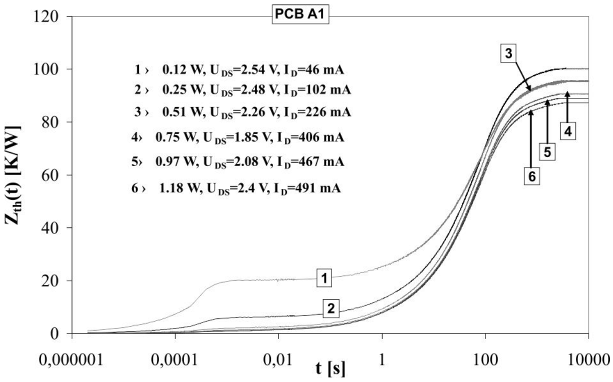

Figure 3: The measured waveforms of transient thermal impedance of the transistor mounted on PCB A1

Table 1: The values of transient thermal impedance model parameters of the transistor mounted on PCB A1

P [W]	0.12	0.51	1.18
R_{th} [K/W]	95.34	95.56	87.37
a_1	0.107	0.121	0.093
τ_{th1} [s]	738.7	631.6	866
a_2	0.471	0.597	0.572
τ_{th2} [s]	99.33	90.25	103.1
a_3	0.136	0.161	0.208
τ_{th3} [s]	17.36	15.27	21.2
a_4	0.049	0.06	0.069
τ_{th4} [s]	2.33	2.21	2.78
a_5	0.023	0.033	0.036
τ_{th5} [ms]	387.2	359.1	473.2
a_6	0.17	0.015	0.011
τ_{th6} [ms]	0.27	1.3	17.33
a_7	0.044	0.013	0.011
τ_{th7} [μs]	40	40	40

As seen, thermal resistance is a decreasing function of the dissipated power and has the values of the range from 90 to 100 K / W. A number of thermal time constants does not depend on the dissipated power and is equal to 7. The thermal time constants have the values of the range from 40 μs to 866 s.

The measurement results of transient thermal impedance of the transistor mounted on various PCBs at the constant dissipated power equal to 0.9 W are presented in Fig. 4. The values of $Z_{th}(t)$ model parameters for the measurement results (Fig. 4) are presented in Table 2.

As seen in Fig. 4, the highest value of thermal resistance is obtained for the transistor operating without the PCB (A0), whereas the value of thermal resistance for the transistor operating on the PCB A2 is about twice lower. Comparing the $Z_{th}(t)$ waveforms of the transistor mounted on the PCB A1 and mounted on the PCBs A2 and A3 it is observed, that the increase of copper area results in a decrease of thermal resistance, whereas the time required to achieve the steady state increases. This is caused by increasing heating capacity due to an increase of the volume of copper. Analysing the contents of Table 2, the correlation between the increase of thermal resistance and the decrease of the longest thermal time constant τ_{th1}, is observed. The values of the thermal time constant τ_{th1} vary within the range from more than 120 s to nearly 900 s.

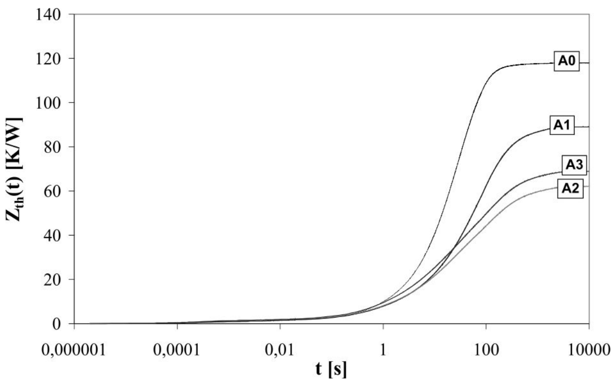

Figure 4: The measured waveforms of transient thermal impedance of the transistor mounted on various PCBs

Table 2: The values of transient thermal impedance model parameters of the transistor mounted on various PCBs

P [W]	A0	PCB A1	PCB A2	PCB A3
R_{th} [K/W]	118	89.03	62.1	68.93
a_1	0.106	0.112	0.122	0.116
τ_{th1} [s]	129.6	682.9	899.4	889.3
a_2	0.772	0.604	0.389	0.385
τ_{th2} [s]	29.71	92.25	127.9	127.1
a_3	0.072	0.168	0.294	0.278
τ_{th3} [s]	4.25	16.42	17.58	17.43
a_4	0.034	0.063	0.106	0.133
τ_{th14} [s]	0.648	2.35	3	2.96
a_5	0.014	0.032	0.052	0.055
τ_{th5} [ms]	1.13	415.3	483.4	473.8
a_6		0.022	0.012	0.012
τ_{th6} [ms]		12.89	24.36	16.09
a_7		0.01	0.021	0.018
τ_{th7} [μs]		40	470	380

The influence of the dissipated power as well as the mosaic design of the PCB on thermal resistance R_{th} of the transistor, is presented in Fig. 5.

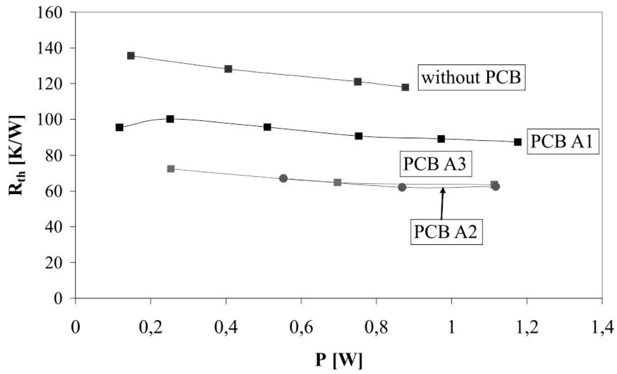

Figure 5: The measured dependencies of thermal resistance versus the dissipated power for different mounting methods of the transistor

The decreasing dependence of thermal resistance on the dissipated power is observed both for the transistor operating without the PCB (A0) and for the transistor mounted on each PCB (A1, A2, A3), due to an increase of convection efficiency resulting from a case temperature rise of the transistor. The strongest dependence $R_{th}(p)$ is observed for the transistor operating without any PCB, because an increase of the dissipated power leads to the most significant temperature rise of the transistor. Thermal resistance of the transistor decreases in the considered range of the dissipated power by even dozen percent.

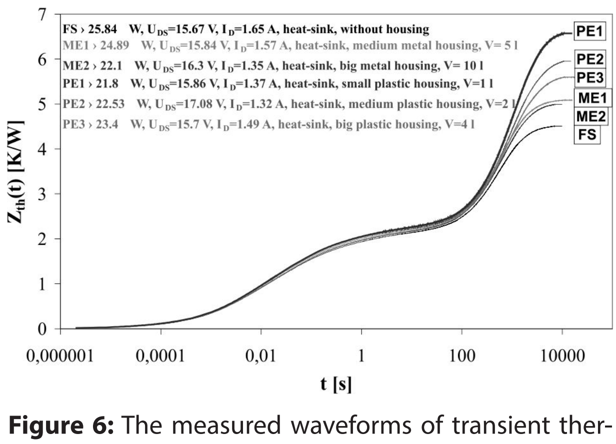

Figure 6: The measured waveforms of transient thermal impedance of the transistor mounted on the heat-sink and enclosed in various housings

The commonly used method for reducing thermal resistance of the semiconductor device is mounting the device on the heat-sink. The measurements performed by the authors show [31] that thermal resistance is a decreasing function of the length of the heat-sink and also depends on the spatial orientation of the heat-sink [32]. Typically, the semiconductor device, however, does not operate individually, but is a part of an electronic device that is enclosed in a housing made of metal or plastic of the defined volume. Figure 6 shows the measured transient thermal impedance of the considered MOS transistor mounted on the heat-sink and placed inside different housings. Designations used in Fig. 6 are discussed in detail in section 3. The values of $Z_{th}(t)$ model parameters for the measurements results (Fig. 6) are presented in Table 3.

As seen in Fig. 6, the measured waveforms of transient thermal impedance $Z_{th}(t)$ of time < 0.1 s for various housings are generally indistinguishable. This is due to the fact that in the initial phase of the transistor cooling, responsibility for the heat dissipation rests with the physical processes occurring inside the transistor as well as on the border between the transistor case and the heat-sink. The smallest value of thermal resistance is for the transistor operating on the heat-sink without housing. Value of the considered parameter increases with decrease of the housing volume. Apart from this, the use of metal enclosure results in the lower value of R_{th} in comparison to the plastic one. The differences in the value of R_{th} for all the considered cooling conditions exceed even 35%. Also, the time t_{ss} required to obtain the thermally steady state in the transistor increases with an increase of thermal resistance. The time t_{ss} for the transistor operating on the heat-sink inside the smallest plastic enclosure (PE1) is about twice grater than for the transistor operating on the heat-sink without the housing.

The influence of the enclosure material and volume on the thermal model parameters is visible due to various conductivity values of the materials used in the construction of enclosure as well as various effectiveness of convection at the surface of the housing.

5 Conclusions

The paper presents experimental results concerning the influence of the cooling system construction of SMD MOSFET on the transient thermal impedance model parameters. Decreasing dependence of thermal resistance on the dissipated power and the area of solder pads, known from the previous work of the authors [23, 31], was confirmed. In addition, mounting the transistor inside the housing, even of a large volume, results in an increase of thermal resistance, whereas the influence of the housing volume on time of determining the internal transistor temperature is ambiguous.

Metal housing, which conducts heat between its interior and the surrounding, provides better cooling that the plastic one. Differences in thermal resistance between the housings made of different materials reach 10%. Mounting the transistor on the PCB can improve cooling efficiency even twice. Mounting the transistor on the heat-sink results in even a 15 times decrease of thermal resistance.

Table 3: The values of transient thermal impedance model parameters of the transistor mounted on the heat-sink and enclosed in various housings

P [W]	FS	ME1	PE2	PE3	ME2	PE1
R_{th} [K/W]	4.51	5.09	5.96	5.6	4.99	6.57
a_1	0.253	0.295	0.498	0.28	0.237	0.381
τ_{th1} [s]	1212.2	1337.3	887	2178.5	1558.2	2034.8
a_2	0.281	0.275	0.078	0.326	0.328	0.274
τ_{th2} [s]	381	417	186.8	554.9	451.1	626.9
a_3	0.051	0.04	0.05	0.02	0.042	0.026
τ_{th3} [s]	2.47	3.49	1.92	16.9	3	6.553
a_4	0.078	0.068	0.078	0.048	0.068	0.049
τ_{th4} [ms]	307.5	425.5	243.5	1345	370.4	660
a_5	0.131	0.12	0.113	0.082	0.122	0.087
τ_{th5} [ms]	47.61	59.68	41.13	168.9	55.98	87.81
a_6	0.12	0.112	0.108	0.117	0.115	0.107
τ_{th6} [ms]	7.26	9.14	6.88	26.72	8.5	12.11
a_7	0,061	0,065	0,053	0,082	0,059	0,053
τ_{th7} [ms]	1,26	1,54	1,2	3,74	1,5	1,71
a_8	0,025	0,025	0,022	0,095	0,068	0,059
τ_{th8} [µs]	40	40	40	60	210	170

The number of thermal time constants increases with the number of elements in the heat-flow path. The thermal model describing the transistor soldered to the wires contains only 4 thermal constants. The number of thermal constants for the transistor mounted on the heat-sink and operating in the housing, however, is even equal to 8.

As seen from the measurements of $Z_{th}(t)$ presented in section 4, the influence of the enclosure unit and area of copper on the PCB, results in a visible change in the instantaneous values of $Z_{th}(t)$ for times exceeding a few seconds. Thus, in construction of the thermal model of a semiconductor device together with its cooling system, it is recommended to use the nonlinear RC Cauer structure [2], wherein each of the heat flow path elements are represented by the two-terminal RCs. Using such structure it is easy to take into account all elements of the heat flow path.

6 Acknowledgements

This project is financed from the funds of the National Science Centre which were awarded on the basis of the decision number DEC-2011/01/B/ST7/06740.

7 References

1. Zarębski J., Górecki K.: The electrothermal large-signal model of power MOS transistors for SPICE. IEEE Transaction on Power Electronics, Vol. 25 , No. 5-6, 2010, pp. 1265 – 1274.
2. Górecki K., Zarębski J.: Nonlinear compact thermal model of power semiconductor devices. IEEE Transactions on Components and Packaging Technologies, Vol. 33, No. 3, 2010, pp. 643-647.
3. Zarębski J., Górecki K.: SPICE-aided modelling of dc characteristics of power bipolar transistors with selfheating taken into account. International Journal of Numerical Modelling Electronic Networks, Devices and Fields, Vol. 22, No. 6, 2009, pp. 422-433.
4. Székely V., Thermal Testing and Control by Means of Built-in Temperature Sensors. Electronics Cooling, Vol. 4, 1998, No. 3, pp.36-39.
5. Székely V., Rencz M., Courtois B., Thermal Investigations of IC's and Microstructures. Microelectronics Journal, Vol. 28, 1997, No.3, pp. 205-207
6. Castellazzi A., Gerstenmaier Y.C., Kraus R., Wachutka G.K.M.: Reliability analysis and modeling of power MOSFETs in the 42-V-PowerNet, IEEE Transactions on Power Electronics, Vol. 21, 2006, No. 3, pp.603-612
7. Reynolds F.H., Measuring and modeling integrated circuit failure rates. Eurocon'82, Copenhagen: Reliability in Electrical and Electronic Components and Systems. North Holland, Vol. 1, 1982, pp. 36-45
8. Parry J., Rantala J., Lasance C.: Temperature and reliability in electronics systems – the missing link. Electronics Cooling, Vol. 7, No. 4, 2001, pp. 30 – 36
9. Ciappa M., Carbognami F., Cora P., Fichtner W.: A novel thermomechanics-based lifetime prediction model for cycle fatigue failure mechanisms in power semiconductors. Microelectronics Reliability, Vol. 42, 2002, pp.1653-1658
10. Castellazzi A., Kraus R., Seliger N., Schmitt-Landsiedel D.: Reliability analysis of power MOSFET's with the help of compact models and circuit simulation. Microelectronics Reliability, Vol. 42, 2002, pp.1605-1610
11. Coquery G., Carubelli S., Ousten J.P., Lallemand R.: Power module lifetime estimation from chip temperature direct measurement in an automotive traction inverter. Microelectronics Reliability, Vol. 41, 2001, pp.1695-1700
12. Happer C.A.: Electronic packaging and interconnection handbook *McGraw-Hill Handbooks, 2000.*
13. Lidow A., Knzer D., Sheridan G., Tam D.: The Semiconductor Roadmap for Power Managment in the New Millennium. *Proceedings of the IEEE*, Vol. 89, 2001, No. 6, pp. 803-812.
14. Sarno C., Moulin G.: Thermal management of highly integrated electronic packages in avionics applications. Electronics Cooling, Vol. 7, No. 4, 2001, pp. 12-20
15. Raj E., Lisik Z., Fiks W.: Influence of the manufacturing technology on microchannel structure efficiency. Materials Science and Engineering B, Vol. 176, No. 4, 2011, pp. 311-315.
16. Gould C.A., Shammas N.Y.A., Grainger S., Taylor I.: Thermoelectric cooling in microelectronic circuits and waste heat electrical power generation in a desktop personal computer. Materials Science and Engineering B, Vol. 176, No. 4, 2011, pp. 316-325.
17. Simons R.E.: Estimating temperatures in a water – to – air hybrid cooling system. Electronics Cooling, Vol. 8, No. 2, 2002, pp. 8-9
18. Garimella S.V., Singhal V., Liu D.: On-chip thermal management with microchannel heat sinks and integrated micropumps. *Proceedings of the IEEE*, Vol. 94, 2006, No. 8, pp. 1534-1548.
19. Zhang H.Y., Pinjala D., Wong T.N., Toh K.C., Joshi Y.K.: Single-phase liquid cooled microchannel heat sink for electronic packages. *Applied Thermal Engineering*, Vol. 25, 2005, No. 10, pp. 1472-1487.

20. Prasher R.: Thermal Interface Materials: Historical Perspective, Status and Future Directions. Proceedings of the IEEE, Vol. 94, No. 8, 2006, pp. 1571-1586.
21. Blackburn D.L.: Temperature Measurements of Semiconductor Devices – A Review. 20th IEEE Semiconductor Thermal Measurement and Menagement Symposium SEMI-THERM, 2004, pp. 70-80.
22. Yener Y., Kakac S.: Heat Conduction.Taylor &Francis, 2008.
23. Górecki K., Zarębski J.: The semiconductor device thermal model taking into account non-linearity and multhipathing of the cooling system. Journal of Physics: Conference Series, Vol. 494, 2014, 012008, doi:10.1088/1742-6596/494/1/012008
24. Carver L.: Innovative packaging design for electronics in extreme enviroments. IEEE Spectrum, No. 5, 2014, pp. S26-S28.
25. Szekely V.: A New Evaluation Method of Thermal Transient Measurement Results. Microelectronic Journal, Vol. 28, No. 3, 1997, pp. 277-292.
26. Górecki K., Rogalska M., Zarębski J.: Parameter estimation of the electrothermal model of the ferromagnetic core. Microelectronics Reliability, Vol. 54, No. 5, 2014, pp. 978-984.
27. Zarębski J., Górecki K.: A New Method for the Measurement of the Thermal Resistance of the Monolithic Switched Regulator LT1073. IEEE Trans. on Instr. and Meas., Vol. 56, No. 5, 2007, pp. 2101-2104.
28. Blackburn D.L., Oettinger F.F., Transient Thermal Response Measurements of Power Transistors. IEEE Transactions on Industrial Electronics and Control Instrum., IECI-22, 1976, No. 2, pp. 134-141
29. Oettinger F. F., Blackburn D. L.: Semiconductor Measurement Technology: Thermal Resistance Measurements, U. S. Department of Commerce, NIST/SP-400/86, 1990.
30. Górecki K., Zarębski J.: The influence of the selected factors on transient thermal impedance of semiconductor devices. Proceedings of the 21st International Conference Mixed Design of Integrated Circuits and Systems MIXDES, 2014, Lublin, pp. 309-314.
31. Górecki K., Zarębski J.: Modeling the influence of selected factors on thermal resistance of semiconductor devices. IEEE Transactions on Components, Packaging and Manufacturing Technology, Vol. 4, No. 3, 2014, pp. 421-428.
32. Górecki K., Zarębski J.: Badanie wpływu wybranych czynników na parametry cieplne tranzystorów mocy MOS. Przegląd Elektrotechniczny, Vol. 85, No. 4, 2009, pp. 159-164.

Arrived: 19. 10. 2014
Accepted: 9. 02. 2015